Unifying the mechanisms for alkane dehydrogenation and alkene H/D exchange with $[IrH_2(O_2CCF_3)(PAr_3)_2]$: the key role of CF_3CO_2 in the "sticky" alkane route

Hélène Gérard,[a] Odile Eisenstein,*[a] Dong-Heon Lee,†[b] Junyi Chen[b] and Robert H. Crabtree*[b]

[a] *Laboratoire de Structure et Dynamique des Systèmes Moléculaires et Solides (CNRS UMR 5636), Université Montpellier 2, 34095 Montpellier cedex 05, France. E-mail: odile.eisenstein@lsd.univ-montp2.fr*

[b] *Department of Chemistry, Yale University, 225 Prospect Street, New Haven, CT 06511-8107, USA. E-mail: robert.crabtree@yale.edu*

Received (in Montpellier, France) 21st February 2001, Accepted 30th May 2001
First published as an Advance Article on the web 21st August 2001

To understand photochemical and thermal alkane activation with $IrH_2(O_2CCF_3)(PAr_3)_2$ (Ar = *p*-FC_6H_4), H/D isotope scrambling between alkenes and $IrD_2(O_2CCF_3)(PAr_3)_2$ was studied. No unique interpretation of the experimental data was possible, so DFT(B3PW91) calculations on the exchange process in $Ir(H)_2(O_2CCF_3)(PH_3)_2(C_2H_4)$ were carried out to distinguish between the possibilities allowed by experiment. Of several possible mechanisms for H/D scrambling, one was strongly preferred and is therefore proposed here. It involves the insertion of the olefin to give an alkyl hydride that reductively eliminates to lead to a transition state that contains an η^3-bound alkane. This transition state, which achieves a 1,1′ geminal H/D exchange, is significantly lower in energy than a dihydrido carbene, located as a secondary minimum, eliminating the alternative carbene mechanism. The unexpectedly large binding energy (BDE) of the alkane ("sticky alkane") to the $Ir(O_2CCF_3)(PH_3)_2$ fragment (BDE = 11.9 kcal mol^{-1}) in this transition state is ascribed in part to the presence of a weakly σ- and π-donating (CF_3CO_2) group *trans* to the alkane binding site. The H/D exchange selectivity observed requires that 1,1′-shifts (*i.e.*, M moving to a geminal C–H bond), but not 1,3-shifts, be allowed in the alkane complex. In a key finding, a 1,3-shift in which the metal moves down the alkane chain is indeed found to have a much higher activation energy than the 1,1′-process and is therefore slow in our system. A 1,2-shift has not been considered since it would involve a strong steric hindrance at a tertiary carbon in this system. The mechanism *via* an alkane path provides an insight into the closely related photochemical and catalytic thermal alkane dehydrogenation processes mediated by $IrH_2(O_2CCF_3)(PAr_3)_2$; the thermal route requires $^tBuCH{=}CH_2$ as the hydrogen acceptor. These two alkane reactions are intimately related mechanistically to the isotope exchange because they are proposed to have the same intermediates, in particular the sticky alkane complex. Remarkably, the rate determining step of the thermal (150 °C) alkane dehydrogenation process is predicted to be substitution of the hydrogen acceptor-derived alkane by the alkane substrate.

Alkane complexes have remained elusive and hard to characterize since alkanes are weak ligands for a transition metal fragment. Such complexes were first inferred from detailed studies of C–H activation processes and related hydrogen isotope scrambling experiments.[1,2] In very early work, alkane complexes were observed at low temperatures for $M(CO)_5$ (M = Cr, Mo, W) fragments in matrices, solution and in the gas phase.[3–5] In spite of the difficulties, some understanding of the behavior of alkane complexes has been acquired.[5–7] Recent flash kinetic studies were carried out on an alkane complex of rhodium.[8] Several proposed organometallic mechanisms require the intermediacy of an alkane complex.[4,9,10] For example, alkane complexes were suggested in several C–H activation reactions,[9] as well as in the substitution of H_2 in an Ir(III) complex[10a] and in the reductive elimination of Tp′RhL(R)(H) (Tp′ = tris-3,5-dimethylpyrazolylborate, L = $CNCH_2CMe_3$).[9c] The culmination of this work has been the recent discovery that some metal fragments can form stable alkane complexes as shown by IR methods,[11] an X-ray determination[12] and NMR measurements.[13,14]

These difficulties in characterization mean that theoretical studies can provide complementary information for identification of reaction paths involving alkane complexes. In several such studies an alkane adduct was proposed as a starting reactant for further chemistry. Several oxidative additions are proposed to start from a weakly bound alkane complex.[15–17] Such an alkane complex (a secondary minimum 3 kcal mol^{-1} above the separated reactants) is found for alkane dehydrogenation catalyzed by (PCP′)$Ir(H)_2$ [PCP′ = 3-$C_6H_3(CH_2PH_2)_2$-1,3].[18] Weak alkane binding was also calculated for $W(CO)_5$.[19] Stronger alkane binding (7–10 kcal mol^{-1} binding energies) was calculated for $[CpM(PH_3)(R)]^+$ (Cp = η^5-C_5H_5; M = Rh, Ir; R = H, CH_3).[18,20] Because of the weak binding, proposals involving alkane intermediates have been avoided if an alternative was available. Computational chemistry now permits a reliable comparison of different reaction paths *via* combined theoretical–experimental studies like the one reported here.

Although many examples of alkane oxidative addition are known,[21] alkane functionalization reactions are still rare.[22–25]

† Present address: Department of Chemistry, School of Natural Sciences, Chonbuk National University, Chonju, 561-756, Korea.

Alkane dehydrogenation catalysis is the longest-known case and we have shown that $[IrH_2(O_2CCF_3)(PAr_3)_2]$ (Ar = p-FC_6H_4) can dehydrogenate alkanes photochemically [eqn. (1)], or thermally [eqn. (2)] in the presence of a hydrogen acceptor such as $^tBuCH{=}CH_2$.[26,27] Isotope exchange has given important information about transient intermediates in organometallic reactions. For example, in $[L_nM(D)(CH_3)]$ (L_nM = Cp*(PMe_3)Ir, Cp_2W, Cp_2Re^+), isotope exchange occurs to give $L_nM(H)(CH_2D)$.[9a,28,29] The intermediacy of alkane complexes of the type $L_nM(CH_3D)$ was proposed, although the intermediacy of carbene complexes $L_nM(=CH_2)(H)(D)$ or $L_nM(=CH_2)(H{-}D)$ could have given the same outcome. Carbene formation would have required Cp slippage to avoid exceeding 18 valence electrons and this possibility was therefore rejected without comment. H exchange in $Cp^*Os(dmpm)(CH_3)(H)^+$ could also be explained by the intermediacy of a carbene or alkane complex[30] but DFT calculations suggested that the latter was more likely.[31] Carbene intermediates explain preferential 1,1-polydeuteration of alkanes by Pt(II)/DOAc in Shilov[32] chemistry.

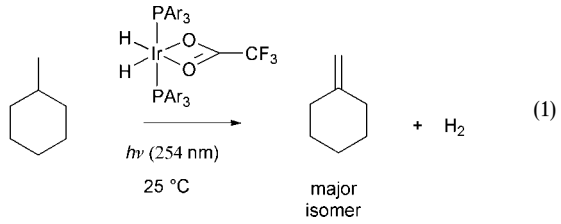

(1)

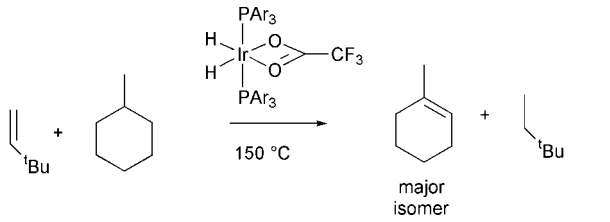

(2)

The goal of this study is to obtain mechanistic information for the alkane dehydrogenation *via* eqn. (1) and (2) from the experimental evidence for the isotope exchange of eqn. (3). The connection between eqn. (1) and (2) and eqn. (3) comes from the more stable dihydrido olefin system of eqn. (3) exploring part of the reaction path of eqn. (1) and (2) in reverse due to the microreversibility principle. We studied and briefly reported H/D isotope exchange data for eqn. (3), the reaction between the hydrogen acceptor $^tBuCH{=}CH_2$ and $[IrD_2(\kappa^2\text{-}O_2CCF_3)(PAr_3)_2]$, but at least two alternate pathways remained possible.[27]

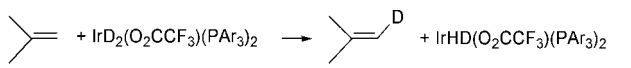

(3)

We originally proposed the intermediacy of a carbene for isotope exchange *via* eqn. (3) since no free alkane was observed and firmly bound ("sticky") alkane complexes were not considered possible at the time; in addition, carbene formation was feasible without ligand slip.[27] The current situation is therefore unsatisfactory in that the same general type of reaction (alkane dehydrogenation chemistry and H/D isotope exchange) currently has two different published explanations.

This paper reports experimental data for the reactions in eqn. (3) and also DFT (B3PW91) calculations that allow us to exclude both carbene[27] and vinylic oxidative addition mechanisms.[33a] We also find faster 1,1′- than 1,3-migration in an alkane complex. A key transition state is found to have an alkane bonded *via* two C–H bonds (η^3) to the metal center. This leads us to propose a *unified* mechanism that accounts both for the isotope exchange in alkenes and for the photochemical or thermal dehydrogenation of alkanes by $[IrH_2(O_2CCF_3)(PAr_3)_2]$.

Results and discussion

Choice of experimental and theoretical systems

Choice of system and synthesis. The Ir(III) complex, $[IrH_2(\kappa^2\text{-}O_2CCF_3)(PAr_3)_2]$ (**1**, Ar = *p*-FC_6H_4) has previously been shown to react with alkanes and alkenes.[26] The d^2-**1** isotopomer is best prepared by reaction of [(cod)Ir-$(PAr_3)_2$](O_2CCF_3) (cod = 1,5-cyclooctadiene) with D_2 for 20 min, but it is also formed from $[IrD_2(PAr_3)_2$-$(O{=}CMe_2)_2]BF_4$ (**2**) and NaO_2CCF_3.

Complex d^2-**1** showed no proton NMR signals in the high-field hydride region but a strong D signal appears at −30.1 ppm in the ^2H NMR spectrum. At incomplete levels of deuteriation, the ^{31}P NMR resonances of all three species, d^0-**1**, d^1-**1** and d^2-**1**, could be distinguished at 22.12, 22.24 and 22.37 ppm as a result of the isotope shifts. The bidentate acetate ligand in **1** is hemilabile, allowing addition of external ligands to give $[IrH_2(\kappa^1\text{-}O_2CCF_3)(L)(PAr_3)_2]$ (**3**, L = CO or η^2-alkene).

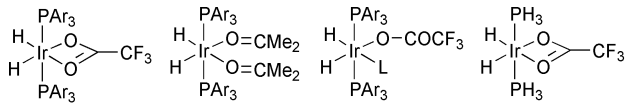

Choice of a computational model. The reaction of $[IrH_2(O_2CCF_3)(PH_3)_2]$ (**4**) and ethylene was studied at the DFT level (B3PW91, see Computational details). When necessary, propene was used as a model olefin. PH_3 was used as a model phosphine, as is usually the case.[17] Unless otherwise mentioned, the reference energy (in kcal mol^{-1}) is that of the separated reactants in their most stable geometry (*i.e.*, **4** with κ^2-coordinated trifluoroacetate, **4κ²**, plus free olefin).

Experimental isotope exchange reactions with 1

Monitoring the reaction mixtures by ^2H NMR spectroscopy over 2 h at 25 °C showed that the deuteriated complex d^2-**1** reacts with a variety of alkenes, leading to isotope exchange with the alkene. Both organic (^2H NMR) and inorganic (^{31}P NMR) products could be monitored. Alkane is a very minor (<5%) product and when this is formed, the resulting reactive $Ir(O_2CCF_3)(PAr_3)_2$ fragment is irreversibly trapped by the solvent to give $Ir(Ph)(H)(O_2CCF_3)(PAr_3)_2$.[33b]

Because disubstituted alkenes $R_2C{=}CH_2$ behave differently, we first consider monosubstituted alkenes such as $PhCH_2$-$CH{=}CH_2$. This shows simultaneous isomerization to the more stable isomer $PhCH{=}CHCH_3$ and D incorporation at all the side chain sites (1, 2 and 3 positions). The isomerization [eqn. (4)] is attributed to a Markovnikov M–D insertion into the C=C bond (M bonded to the more substituted carbon) to give a secondary alkyl, followed by β-elimination; this process labels the 1 position. Concomitant insertion/elimination in an anti-Markovnikov fashion [not shown in eqn. (4)] in the reactant alkene labels the 2 position. Labeling at C-3 can arise from further insertion/elimination. Everything can be interpreted *via* insertion/β-elimination and nothing else is required, so monosubstituted alkenes are not mechanistically useful.

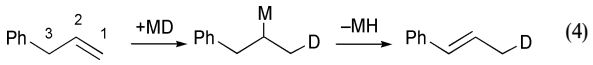

(4)

Disubstituted alkenes, $R_2C{=}CH_2$, in contrast, only show isotope exchange with d^2-**1** at the unsubstituted carbon without significant (<2%) alkene isomerization. For methylenecyclohexane, the endocyclic isomerization product, 1-methylcyclohexene, known to be more stable than the starting alkene, should have been seen if a pathway were available. For isobutene, the isomerization is degenerate, but it would still label the methyl groups; this did not happen to any significant (<2%) extent.

The reactions described here only occur in hydrocarbon solvents. In halogenated solvents such as CH_2Cl_2, the metal complex degrades by oxidation. In polar solvents like acetone, the CF_3COO^- ligand is displaced and the resulting $[IrH_2(solvent)_2L_2]CF_3COO$ gives quite different chemistry.

Experimental probe of trifluoroacetate coordination

To see if the trifluoroacetate ligand (tfa) in **1** remained bound, we studied the reaction of methylenecyclohexane with $[IrD_2(PAr_3)_2(O{=}CMe_2)_2]BF_4$, d^2-**2**, under identical conditions.[33b] **2** is expected to be a good model for the case in which the tfa completely dissociates since $O{=}CMe_2$ is a good leaving group. In sharp contrast with **1**, **2** gave a very rapid (seconds) isomerization to 1-methylcyclohexene [eqn. (5)]. The 1-methylcyclohexene is deuterium-labeled, principally at the CH_3 group. The tfa in **1** must therefore remain bound, at least under the conditions used, or isomerization of the olefin would have been seen.

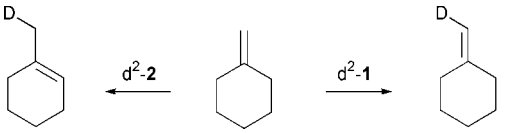

(5)

Experimental observation of intermediate alkene complexes

As reported earlier,[33b] we examined the reactions of the tfa complex, **1**, with alkenes at low temperature by ^1H NMR in an attempt to directly observe reaction intermediates, to help infer the reaction path. In all cases we saw either no change or only the formation of an alkene complex of the type $[IrH_2(\kappa^1\text{-}O_2CCF_3)(L)(PAr_3)_2]$ (**3**, L = η^2-alkene) in equilibrium with the starting complex **1**. These were characterized by ^1H NMR spectroscopy because attempts to isolate them led to reversion to the parent complex **1**. CO did bind more strongly to give **3** (L = CO), isolated as a moderately stable complex. In both cases, ^1H NMR spectroscopic data were consistent with the presence of *cis* hydrides.

Equilibrium constants, also reported earlier,[33b] show steric and electronic effects; small alkenes (*e.g.*, C_2H_4, $K_{eq} > 5 \times 10^3$ L mol^{-1} in CD_2Cl_2 at −80 °C) and those with electron withdrawing groups (*e.g.*, styrene, $K_{eq} = 32$) bind best. As an example of steric effects, ethylene binds strongly but the bulky ^{t}BuCH=CH_2 binds weakly ($K_{eq} = 0.58$). Electronic effects are indicated by the fact that $Me_3SiCH{=}CH_2$ ($K_{eq} = 1.3 \times 10^3$) binds much better than ^{t}BuCH=CH_2 ($K_{eq} = 0.58$) and styrene ($K_{eq} = 32$) binds better than 1-hexene ($K_{eq} = 17$).

Theoretical study of intermediate alkene complexes

Calculations on the model starting complex $[IrH_2(O_2CCF_3)(PH_3)_2]$, **4**, show that the tfa is hemilabile. The bidentate κ^2 and the monodentate κ^1 forms are local minima close in energy on the potential energy surface (PES). **4κ²** is pseudooctahedral while **4κ¹** is a Y-type distorted trigonal bipyramid (TBP)[34–36] with apical phosphines (Fig. 1). **4κ¹** lies only 5.3 kcal mol^{-1} above **4κ²**. This is consistent with an energetically facile opening of **4κ²** to allow the coordination of an incoming ligand.

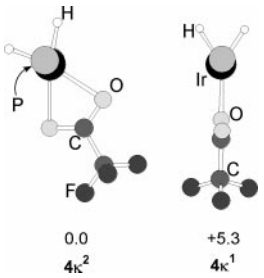

Fig. 1 Optimized structures for type **4** complexes: **4κ¹** right and **4κ²** left. For clarity, the hydrogens of PH_3 are not shown. Energies are in kcal mol^{-1}.

When ethylene binds, two adducts, each with κ^1-tfa and *trans* phosphines, are located as minima (Fig. 2). In line with experiment, the more stable ethylene isomer, **5c** (−16.2 kcal mol^{-1} relative to **4κ²** plus free ethylene), has *cis* hydrides and therefore the olefin is *cis* to tfa (Fig. 2). Isomer **5t** with *trans* hydrides is not observed experimentally, in agreement with its high energy relative to **5c** (+11.4 kcal mol^{-1} above **5c**). In both complexes, ethylene is predicted to be perpendicular to the Ir–P direction. Paradoxically, ethylene is more weakly bound to Ir in the more stable **5c** than in **5t** as indicated by the geometric parameters: longer C=C and shorter Ir–C distances in **5t**. The greater stability of **5c** is thus not associated with stronger olefin binding but with a better mutual arrangement of the two H ligands. With their large *trans* influence, mutually *trans* hydrides as in **5t** are especially unfavorable.

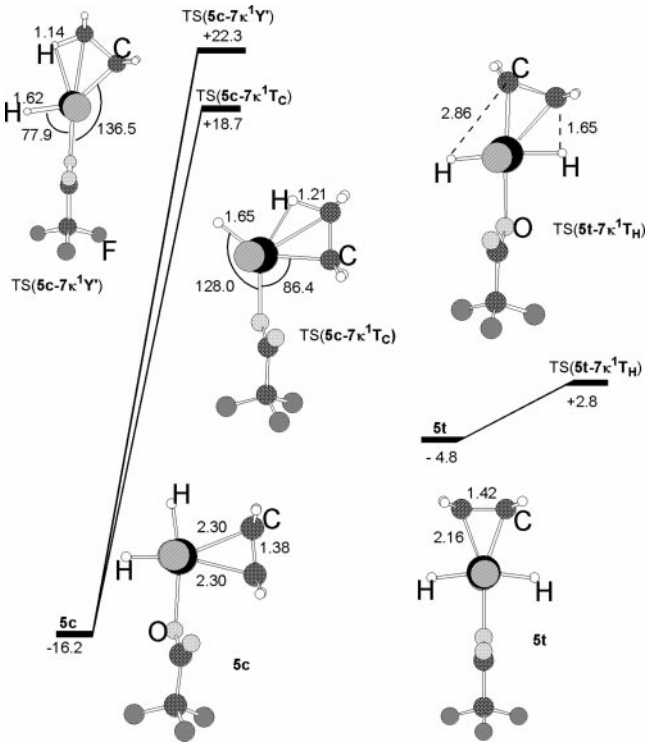

Fig. 2 Reaction paths and optimized structures and transition states (distances in Å, angles in °) for insertion of C_2H_4 into the Ir–H bond for *cis*-$IrH_2(\kappa^1\text{-tfa})(C_2H_4)(PH_3)_2$, **5c** (left) and for *trans* $IrH_2(\kappa^1\text{-tfa})(C_2H_4)(PH_3)_2$, **5t** (right). Hydrogens of PH_3 are not shown for clarity. Energies are given with respect to **4κ²** plus free ethylene (in kcal mol^{-1}).

Experimental study of oxidative addition mechanism

The failure of alkenes of the type $R_2C{=}CH_2$ to isomerize during H/D exchange *could* be explained by an oxidative addition to the vinyl C–H bond, as found experimentally for IrH_5L_2,[33a] so we looked for experimental methods for distinguishing this mechanism (Fig. 3). In the authentic vinyl activation pathway, strong selectivity is seen for exchange of the vinyl C–H *trans* to the bulky ^{t}Bu group and fast exchange also occurs readily with arenes. In contrast, in our system, $IrH_2(tfa)L_2$ at room temperature with *no* added ^{t}BuCH=CH_2, there is no selectivity at all in alkene exchange and arenes are unreactive (<2 h). One could perhaps dismiss the failure to distinguish between the *cis* and *trans* positions of the unhindered terminal CH_2 group, but the highly hindered α-vinyl position of ^{t}BuCH=CH_2 is also attacked equally fast. In methylenecyclohexane, there can be no selectivity, but it does not seem reasonable to postulate a different mechanism for ^{t}BuCH=CH_2 and methylenecyclohexane.

The absence of reaction with arenes in the absence of an H acceptor is especially informative. Arene C–H bonds are very reactive in oxidative addition, so $Ir^{III}H_2(tfa)L_2$ cannot undergo oxidative addition; the required Ir(v) intermediate is expected to be unfavorable. In the reaction of $[IrD_5(PCy_3)_2]$/^{t}BuCH=CH_2 where oxidative addition does occur, this can take place at the Ir(I) level after loss of dihydrogen (Fig. 3).[33a] If the same mechanism is considered in the case of $IrH_2(tfa)L_2$, the loss of H_2 to a sacrificial olefin would lead to $Ir^I(tfa)L_2$, which has *no hydride left* and thus cannot be involved in H/D exchange. This is in full agreement with experimental observations. Under the conditions we use (room temperature, <2 h) and in the absence of a hydrogen acceptor, no significant arene deuteration was observed with benzene or naphthalene.

The $IrH_5(PCy_3)_2$ system shows an induction period during which formation of ^{t}BuEt is observed; neither an induction period nor ^{t}BuEt is seen in our system. The induction period is proposed[33a] to involve hydrogen transfer from Ir to give a coordinatively saturated intermediate, plausibly Ir(I), which gives vinyl oxidative addition. The vinyl activation route might be expected to show a significant primary isotope effect, because although a range of primary isotope effects have been seen for C–H(D) oxidative additions to late transition metals,[37] our particular system [**1** after a long (10 h) induction period] allows the formation of $Ir^I(tfa)L_2$, which can oxidatively add to arene. The Ir(I) intermediate retains a hydride in the coordination sphere of the metal and can therefore give H/D exchange. This system shows[33b] a k_{CH}/k_{CD} of 4.5 for C_6H_6/C_6D_6, attributed to the oxidative addition step. When we ran the reaction in eqn. (3) in reverse mode at room temperature over 2 h, using deuteriated d^2-alkene (formed from Ph_3PCD_2 and cyclohexanone by a standard Wittig reaction)[37b,c] and protonated metal complex, d^0-**1**, with observation by ^{2}H NMR, k_{CH}/k_{CD} was found to be 2.5(±0.1). This value is sufficiently different from that at long reaction times to suggest a different mechanism.

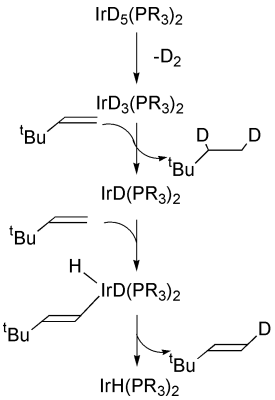

Fig. 3 Reaction mechanism for H/D exchange between CH_2=CH^{t}Bu and IrL_2D_5.[33a]

These are independent, converging arguments that show that the mechanism of H/D exchange by $IrH_2(tfa)L_2$ at room temperature does not allow oxidative addition at the Ir(III) level and does not form (at short times, <2 h) Ir(I)(tfa)L_2, which is capable of oxidative addition. We therefore moved to a theoretical study to compare the possible routes.

Theoretical studies of vinylic oxidative addition to Ir

The experimental results clearly suggest that $Ir(III)H_2(tfa)L_2$, **1**, is unlikely to oxidatively add, even to a reactive C–H bond. We decided to see if the calculations could confirm this point. The C–H oxidative addition to **4κ^1**, to give vinyl $[IrH_3(CH{=}CH_2)(PH_3)_2(\kappa^1\text{-tfa})]$, **6**, was calculated. Two minima, close in energy, differing only in the orientation of tfa, were located for **6** (Fig. 4). They both have *trans* phosphines and an $IrH(H_2)$ ligand set, showing a preference for Ir(III) over Ir(v). The energies are +10.6 (**6a**, tfa eclipsing Ir–P) and +11.5 kcal mol^{-1} (**6b**, tfa perpendicular to Ir–P), respectively, above **4κ^2** plus free ethylene. A third Ir(III) vinyl complex, **6c**, with *cis* phosphine ligands and an IrH(H)(tfaH) ligand set was located 10.4 kcal mol^{-1} above the energy reference. Any mechanism going through these vinylic intermediates is thus unlikely because their energy is significantly higher than that of the separated reagents, **4κ^2** and free ethylene.

To test the role of the anionic ligand in the vinylic C–H activation, we replaced tfa by H. As expected, the vinylic species $[IrH_4(CH{=}CH_2)L_2]$ is a pentagonal bipyramidal Ir(v) tetrahydro vinyl with apical phosphines. Its energy (30.1 kcal mol^{-1} *above* the more stable ethylene complex) shows that this reaction is disfavored. Thus, whatever the anionic ligand, the 5-coordinate Ir(III) fragment does not give vinyl C–H activation.

Initial step: alkene insertion into the Ir–H bond

Insertion of methylenecyclohexane into the Ir–H bond is left as the most likely path. This is expected to be anti-Markovnikov to give the primary alkyl, because the opposite orientation would lead to an unfavorable bulky tertiary alkyl and 1-methylcyclohexene, not seen experimentally, as final products. The labile and less hindered cationic acetone complex **2** does give a Markovnikov insertion, however, because the products of such an alkene isomerization are seen. Since methylenecyclohexene is never seen for **1**, we propose that the very hindered tertiary alkyl intermediate required for isomerization never forms. With this in mind, we did not introduce any substituents into the model compounds because the bulky groups are always remote from the metal.

Ethyl complexes of type **7** result from ethylene insertion into one Ir–H bond in **4**. Several minima close in energy were predicted either with κ^2-tfa (**7κ^2**) or with κ^1-tfa (type **7κ^1**) (Fig. 5). The two **7κ^2** complexes that were located as minima are pseudooctahedral and differ only in the orientation of the

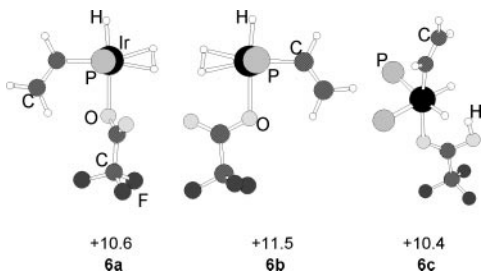

Fig. 4 Optimized structures for type **6** vinyl complexes: **6a**, **6b** and **6c**. For clarity, the hydrogens of PH_3 are not shown. Energies are given with respect to **4κ^2** plus free ethylene (in kcal mol^{-1}).

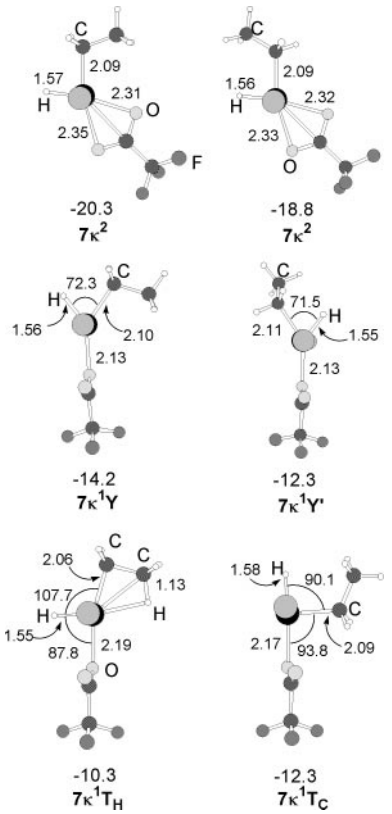

Fig. 5 Optimized structures (distances in Å, angles in °) for type **7** alkyl complexes Ir(H)(tfa)(C_2H_5)(PH_3)$_2$. For clarity, the hydrogens of PH_3 are not shown. Energies are given with respect to **4κ²** plus free ethylene (in kcal mol^{-1}).

ethyl ligand; they are 4.1 and 2.5 kcal mol^{-1} below the most stable ethylene complex **5c**. All 16-electron **7κ¹**-type complexes are calculated to be less stable than the 18-electron **7κ²** species although the energy difference is not large for hemilabile tfa. In the complexes with κ¹-tfa and *trans* phosphine ligands, the three other ligands can form either a square pyramid (T) or distorted TBP (Y) arrangement (Fig. 5).[34–36] Two complexes were found with a Y arrangement, tfa occupying the foot of the Y, at 2.0 (**7κ¹Y**) and 4.0 kcal mol^{-1} (**7κ¹Y′**) above **5c**; they differ only by rotation about the Ir–C_α bond and the ethyl group is not agostic. Two T-shaped alkyls were also found with hydride, **7κ¹T$_H$**, or alkyl, **7κ¹T$_C$**, *trans* to the vacancy at 5.9 and 3.9 kcal mol^{-1} above **5c**, respectively. The former, **7κ¹T$_H$**, forms a β-agostic C–H structure (Ir–C_α–C_β = 90.7°; C_β–H = 1.13 Å). This interaction appears to be weak since removing it by rotating around the C_α–C_β bond while keeping the angles between the ligand bond at the metal as in the agostic complex does not significantly alter (0.2 kcal mol^{-1}) the energy of **7κ¹T$_H$**. The similarity of the energies found for the Y- and T-shaped alkyl complexes confirms prior studies showing the high fluxionality of d^6 ML_5 complexes[36] and suggests interconversion between the different alkyl minima is easy with monodentate κ¹-tfa.

The search for the transition state (TS) for the insertion of the ethylene into the Ir–H bond gave remarkable results. No TS could be found that links any olefin complex of type **5** to the 18-electron **7κ²** alkyl complex. All transition states located link an olefin complex (type **5**) to an ethyl complex with monodendate tfa (type **7κ¹**). A TS, denoted **TS(5c-7κ¹Y′)** was found between the ethylene complex with *cis* hydrides **5c** and the Y-shaped **7κ¹Y′** (Fig. 2, left). Likewise, **TS(5c-7κ¹T$_C$)** was also located (Fig. 2, middle). These two transition states, which are 38.5 and 34.9 kcal mol^{-1} above **5c**, respectively, are too high to be reachable, being more than 18 kcal mol^{-1} above the separated reactants. The lowest energy insertion path goes from the *less* stable and experimentally unseen *trans* hydride ethylene complex, **5t**, to the agostic alkyl, **7κ¹T$_H$** *via* **TS(5t-7κ¹T$_H$)**, only 7.6 kcal mol^{-1} above **5t** (Fig. 2, right). In going from **5t** to **TS(5t-7κ¹T$_H$)**, one of the hydrides approaches the ethylene (C_β···H 1.65 Å) and the other hydride moves away (C_α···H 2.86 Å). One reason why insertion of ethylene is so easy from **5t** is the higher nucleophilicity of the hydride *trans* to another hydride. A hydride *trans* to a weak *trans* effect ligand like tfa is expected to be much less nucleophilic. Another factor also helps to lower the transition state from the less stable olefin isomer. Starting from **5c** the new σ Ir–C bond necessarily develops pseudo *trans* to the remaining hydride (Fig. 2); having two high *trans* effect ligands mutually *trans* is unfavorable. When inserting from the less stable olefin complex, **5t**, the new Ir–C bond develops *cis* to Ir–H, a more favorable situation. The ethylene complex that is both experimentally observed and predicted to be most stable is thus a dead-end for the reaction since the insertion is energetically inaccessible from this isomer and the whole reaction is proposed to go through the less stable ethylene adduct **5t**. Related results were previously calculated for the reaction of ethylene with (PCP′)Ir(H)$_2$ [18] and for $RhH_2(Cl)(C_2H_4)$.[15,16] This shows a sigificant influence of the ancillary ligands on the insertion of an olefin into a metal–hydride bond.

Pathway for H/D exchange

In the methylenecyclohexane and the isobutene cases, after the insertion takes place to give the primary alkyl, the elimination has to occur *via* the removal of the same D label originally added to the alkene in the insertion step because no alternative is available. This would lead to the formation of unlabeled alkene and so does not explain our observation of label incorporation. Two leading mechanisms need to be considered for the isotope exchange, one involving an alkane complex (modeled later by **8**) and the other a carbene intermediate (modeled later by **9**) (Fig. 6). In the carbene pathway, α-elimination causes exchange between Ir–D and the α-CH_2 group of the alkyl *via* a carbene intermediate. In the alkane pathway, the H/D exchange takes place *via* reductive elimination to give an alkane complex in which the metal then migrates from one CH bond to a geminal one. These are not readily distinguishable experimentally, hence the need for theory. As shown in Fig. 6, we expect the alkene product to be labeled with a single D in either mechanism, in line with experiment since we find that the majority (>90%) of the labeled isobutene formed contains just one and not two deuteriums per molecule.

Carbene complex as intermediate

In the carbene path, fast α-elimination to give a carbene dihydride or dihydrogen complex allows H/D exchange by a reverse α-migration to regenerate the alkyl, now deuterium labeled. A β-elimination step completes the process and introduces one D per molecule, as observed. This pathway seemed the most reasonable to us in the early work and we initially suggested it for the isotope exchange.[27]

The β-elimination of a transition metal alkyl and its reverse reaction, 1,2-insertion of an alkene into an M–H bond, are very common. Much rarer are α-elimination of an alkyl and its reverse, 1,1-insertion of a carbene into an M–H bond, about which relatively little is known.[38–40] Attention has been drawn to this problem following several significant results. Schrock and co-workers[38a] reported a series of paramagnetic Mo(IV) alkyls where α-elimination is $>10^6$ times faster than β-elimination. Other early transition metal cases involve rapid α-elimination. Among the late transition metals, a tetracoordinate 14e Ru hydride reacts with a vinyl hydride to give a Fischer carbene hydride [eqn. (6)]. DFT calculations of the reaction path for an ethylene model ligand suggests a multi-

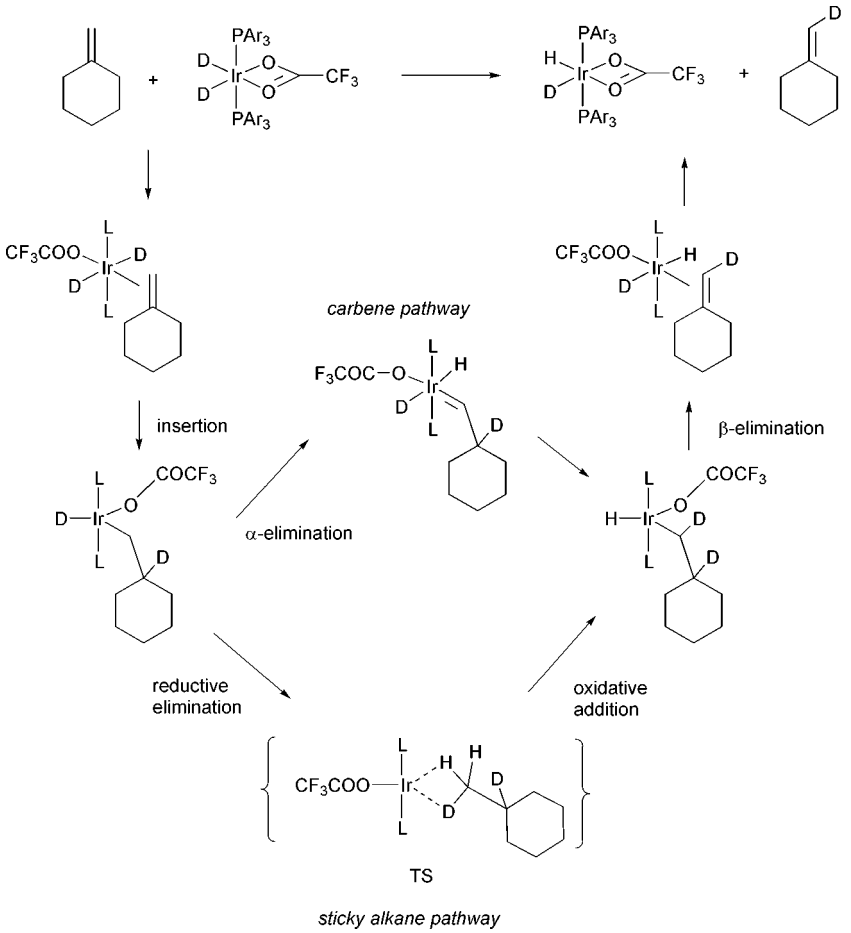

Fig. 6 The mechanism for H/D exchange in methylenecyclohexane *via* the carbene and the alkane routes. The structures shown are schematic and are not intended to represent preferred geometries. The alkane pathway is proposed in this work. The species in curly brackets may not be a stable minimum.

step path involving insertion to form an alkyl that rearranges to the final carbene hydride by α-elimination.[39,40]

$$HRuClL_2 + CH_2{=}CH(OEt) \rightarrow RuClL_2[CHMe(OEt)] \rightarrow HRuClL_2[{=}CMe(OEt)] \quad (6)$$

In pursuit of this alternate mechanism for the present system, three dihydride carbene complexes (type **9**) with monodentate tfa were located as minima on the PES (Fig. 7). No minimum with bidentate tfa or dihydrogen ligands could be located. The two minima with *trans* phosphines have either *cis* hydrides (carbene **9c**, 12.9 kcal mol^{-1} above **4κ²** plus ethylene) or *trans* hydrides (carbene **9t**, 7.3 kcal mol^{-1} above **4κ²** plus ethylene). Thus, unlike the ethylene case, the carbene

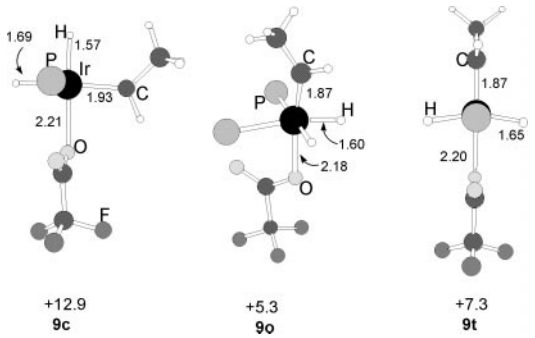

Fig. 7 The optimized structures (distances in Å) of the carbene dihydride complex Ir(tfa)(CH=CH$_2$)(PH$_3$)$_2$. For clarity hydrogens of PH$_3$ are not shown. Energies are given with respect to **4κ²** plus free ethylene (in kcal mol^{-1}).

complex is predicted to be more stable with *trans* (**9t**) than with *cis* hydrides (**9c**). A more stable carbene isomer, **9o**, with *cis* phosphines was located 5.3 kcal mol^{-1} above separated **4κ²** and ethylene. Even though PAr$_3$ is not very bulky and *cis* arrangements are known in closely related cases,[41] **9t** probably lies very close in energy to **9o** and could be preferred when steric effects are considered. For this reason only **9t** will be considered below as representing the carbene complex. The transformation of the more stable ethylene adduct **5c** into the carbene complex **9t** is thus endothermic by 23.5 kcal mol^{-1} (12.1 kcal mol^{-1} above the less stable **5t** isomer). High endothermicity was also calculated for other metal fragments: RuHCl(PH$_3$)$_2$ (16.0 kcal mol^{-1})[39,40] and RuH(CO)(PH$_3$)$_2$ (23.4 kcal mol^{-1}).[42] The carbene being unlikely, we turn to the alternate alkane pathway for H/D exchange.

The alkane route

Free alkane is not a significant product (<5%), so any Ir(I)–alkane species must be stable enough to prevent alkane dissociation before C–H oxidative addition takes place. Once the alkane species forms, the metal has to undergo facile 1,1′-migration of the alkane ligand so the initial Ir–(D–CH$_2$R) alkane species becomes Ir–(H–CHDR). The subsequent steps reverse the previous ones: a C–H oxidative addition to give the alkyl hydride Ir(III) complex is followed by a β-H-elimination to yield the final labeled alkene (Fig. 6).

Calculations support the alkane mechanism. The alkane complex **8** was found to be square planar with a side-on η^2-alkane (Fig. 8) located 0.9 kcal mol^{-1} below separated **4κ²** plus ethylene. The binding energy of the ethane is large (14.4 kcal mol^{-1}), consistent with the significant elongation of the

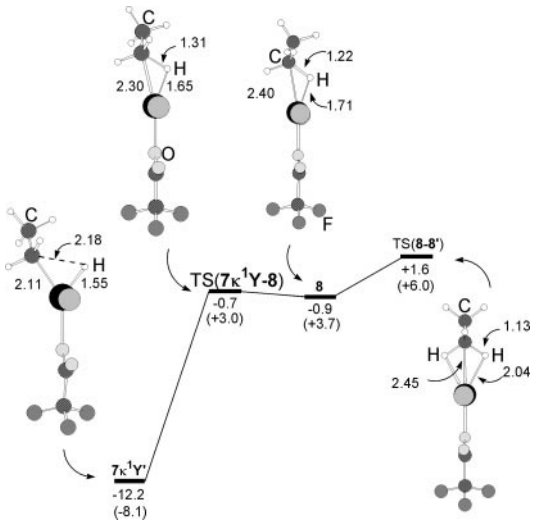

Fig. 8 The reaction path for hydride exchange in the alkyl complex $Ir(H)(C_2H_5)(tfa)(PH_3)_2$ *via* the alkane route (distances in Å). For clarity, the hydrogens of PH_3 are not shown. Energies (including ZPE in parentheses) are given with respect to **4κ²** plus free ethylene (in kcal mol^{-1}).

C–H bond from 1.10 Å in free C_2H_6 to 1.22 Å in the alkane complex. The large binding energy contrasts with the usual weak binding to transition metals[4,9,10,18,25,43] but is supported by recent observations of moderately stable alkane complexes.[12–14] Entropy effects cannot be computed quantitatively in the harmonic approximation, but these should lower the ΔG of binding. The calculated ΔG of dissociation ($+2.3$ kcal mol^{-1}) should therefore only be viewed as a further indication that alkane should not be lost easily.

Formation of the alkane complex starts with reductive coupling (reductive elimination of alkyl and hydride in which the alkane remains bound to the metal). The starting alkyl **7κ¹Y′** is proposed to go to the alkane complex, **8**, *via* a transition state **TS(7κ¹Y′-8)** only 0.2 kcal mol^{-1} above **8** (Fig. 8). The TS geometry naturally greatly resembles that of **8**, with the exception of small changes in the Ir–C–H region. As expected, the C–H bond is longer and the Ir–C and Ir–H bonds are shorter in **TS(7κ¹Y′-8)** than in **8**. Significantly, the reductive coupling starts from a Y-shaped alkyl complex having a short distance between the alkyl and H to be coupled. This Y complex is easily obtained from any T structure owing to the well known flatness[36] of the PES for d^6 ML_5 species. It is probably for this reason that we were unable to locate a transition between **7κ¹T$_H$** and **7κ¹Y′**. Faster reductive elimination from low coordinate organometallic species is a common finding; the greater flexibility of these intermediates may allow distortions that lead to the appropriate transition states.

The isotope exchange cannot be completed without 1,1′-exchange within the alkane complex, converting C–D–M to C–H–M so that D is retained in the alkene. The TS for 1,1′-exchange, **TS(8-8′)**, with C_s symmetry and two C–H bonds proximate to the metal, is located only 2.5 kcal mol^{-1} above **8** (prime labels describe structures equivalent to non-prime labels after H exchange). In this η^3-ethane species, the two C–H bonds are moderately stretched to 1.13 Å (Fig. 8). In **TS(8-8′)** the alkane is still strongly bound (11.9 kcal mol^{-1}), allowing the H/D exchange to occur without formation of free ethane. The activation energy for this exchange is very close to that calculated in $CpOs(dmpm)(CH_3)H^+$ (2.0 kcal mol^{-1}).[31] The highest *transition state* of the alkane path is **TS(8-8′)**, which is at lower energy than the *intermediates* in the carbene path. If so, this leads to the conclusion the that the alkane path is most likely for the isotope exchange.

The small predicted energy difference between **TS(7κ¹Y′-8)** and alkane complex **8** makes the existence of the alkane complex questionable as a distinct intermediate (Fig. 8). Adding the zero point energy (ZPE) to the total energies reverses their relative stabilities with **TS(7κ¹Y′-8)** now being 0.7 kcal mol^{-1} below **8**. The shape of the PES involving **TS(7κ¹Y′-8)** and the alkane complex **8** was thus computed with another functional. With B3LYP, the alkane bonding dissociation energy (BDE) is 11.3 kcal mol^{-1}, consistent with its shorter (1.18 Å) C–H bond (B3PW91: 1.22 Å). For comparison, free C_2H_6 has a C–H distance of 1.095 Å with both methods. With B3LYP, **TS(7κ¹Y′-8)** is 1.4 kcal mol^{-1} above **8** without ZPE. Including ZPE with B3LYP (this functional will no longer be used in what follows) results in the two species having essentially the same energy (difference of 0.1 kcal mol^{-1}). Consequently, the pathway for the reductive coupling of the alkyl group and H followed by a 1,1′-exchange of hydrogens is best described as a concerted C–H bond metathesis in the alkyl complex. The transition state for 1,1′-exchange, **TS(8-8′)**, has the character of a chelated alkane complex with two short C_α–H bonds (B3PW91: 1.13 Å) bound to the metal and with an sp^3 C_α center (H–C–H = 112.0°). The H/D exchange should still be considered as going *via* an alkane-type transition state, **TS(8-8′)**. Precisely this kind of 1,1′-shift has been proposed to explain the NMR spectrum of the alkane complex, $CpRe(CO)_2$(cyclopentane).[13,14]

Further insight into the alkane path

Special role of the tfa ligand. Even though the η^2-bonded alkane is at best a very shallow secondary minimum, it is convenient to consider for discussion purposes. The tfa ligand has a central role in enhancing the binding energy of ethane to $Ir(\kappa^1\text{-tfa})(PH_2)_2$. Replacing tfa by H lowers the predicted binding energy to 5.2 kcal mol^{-1} and shortens the C–H bond to 1.13 Å. The binding energy is thus larger for tfa than for H since tfa is an electronegative ligand with weak *trans* influence and some π-donating ability. The C–H–metal interaction can also be quantified by examining the agostic C–H vibration frequencies. Binding to the metal weakens the C–H bond. The average calculated ν_{C-H} of the free C–H in the ethane complex is 3114 cm^{-1} (± 40 cm^{-1}) whereas the ν_{C-H} frequency of the metal-bound C–H is lowered to 1722 cm^{-1}. Replacing tfa by H raises ν_{C-H} of the η^2-bonded C–H to 2624 cm^{-1}, in agreement with the shorter C–H distance.

Comparison with previous calculations of alkane complexes highlights some important features. Prior discussions have emphasized the hapticity,[19,44] the role substituents,[19] and the solvent.[17,45] Binding energies and geometries not only depend on the metal and ligand but also on the level of calculations. Alkane complexes have been calculated for metals with various electron counts (d^2, d^6, d^8, d^{10}). Bound alkanes in d^{10} complexes have very low bond dissociation energies (<5 kcal mol^{-1}) and very small C–H elongations (C–H < 1.11 Å).[46,47] Coordinated alkane in d^6 and d^8 complexes have larger M–alkane BDEs, which vary significantly with the level of calculations. For instance, the BDE of CH_4 in $M(Cp)(CO)^q$ (M = Os, $q = -1$) is only 10.1 kcal mol^{-1} at the B3LYP level but 9.3 kcal mol^{-1} larger at the MP2 level.[48] Changing the correlation functional in hybrid DFT methods from B3LYP to B3P86 increases the BDE by nearly 5 kcal mol^{-1} in the same type of compound (M = Ir, $q = 0$).[49] Similar variations have been calculated in this work for $Ir(tfa)(PH_3)_2(C_2H_6)$, with B3LYP giving a lower BDE than B3PW91.

Ligands greatly influence the alkane BDEs. Methane binding energies to $Ir(PH_3)_2X$ (X = H, Cl), calculated at the RHF level are 6.8 (X = H) and 15.6 kcal mol^{-1} (X = Cl).[50] Replacing H by Cl thus has similar effects to those found on replacing H by tfa in this work. Both tfa and Cl have a lower σ-donor ability than H and both lead to a larger alkane BDE. The RHF level also reproduces the lowering of the ν_{C-H},

larger for Cl than for H, although the extent of this lowering is much smaller at the RHF level than at the B3PW91.

1,*n*-Shifts ($n = 1$ to 3) in agostic alkane complexes. Although 1,1′-migration of Ir in the alkane complex has to be fast, neither 1,2- nor 1,3-migration of the metal in the proposed alkane complex can be fast because these processes would lead to net alkene isomerization, which is not observed. Since the H atoms of an alkane are essentially close packed around the carbon core, this restriction initially seemed unreasonable and originally led us to disfavor the alkane complex pathway. Fast 1,1′- *vs.* 1,2- and 1,3-migration must apply to our case and has been seen in NMR data on alkane complexes,[13,14] but, as Periana and Bergman have shown,[9a] some alkane complexes can undergo 1,2- and 1,3-shifts. Because all the alkane complexes in this paper with slow 1,2- and 1,3-migration are derived from disubstituted alkenes, all have tertiary C–H bonds adjacent to the C–H bond formed by reductive coupling. Coordination through the tertiary C–H bond could be strongly disfavored because the bulky R groups might hinder the required side-on binding, which could well prevent a 1,2-shift from occurring. Calculations on propane *vs.* ethane show that one additional methyl group on C_α decreases the alkane binding energy by 2.4 kcal mol^{-1} whereas it has no influence when substituted at C_β. This trend is thus opposite from that calculated for $W(CO)_5$(alkane)[19] but energy variations in the latter unhindered system were too small to be conclusive. No further calculations were thus carried out on the 1,2-shift.

The TS for 1,3-migration of the metal on propane was found to be 11.7 kcal mol^{-1} above the primary propane complex and only 2.9 kcal mol^{-1} below the dissociation of propane. No direct 1,3-shift is thus expected to occur. In this poorly bonded transition state, the hydrogens of the two C–H bonds are pointing directly toward the metal in a chelated $\eta^1 + \eta^1$ mode, quite unlike the usual side-on η^2 arrangement of the σ-bonded alkane. We interpret the high barrier of the 1,3-shift *vs.* the 1,1′-shift to mean that decoordination of the metal from the carbon of the C–H bond, required for the 1,3- but unnecessary for 1,1′-shift, is unfavorable in this case (**10**).

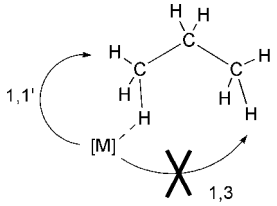

10

Alkane as protecting group. The calculations suggest that when X is tfa, the alkane acts as a protecting group for the highly reactive $\{IrXL_2\}$ fragment, which would otherwise undergo oxidative addition[17,20] with an external substrate or *via* orthometallation. This protection is effective at 25 °C but on heating, the alkane departs because the thermal (150 °C) alkane dehydrogenation system does give both alkane and arene CH activation. When X is H, the weakly bound alkane is no longer a protecting group. This protection is especially important against vinylic oxidative addition with the 14-electron tricoordinate Ir^IXL_2. The vinylic oxidative addition, calculated to be thermodynamically favorable with the two anionic ligands, will be presented in a future paper.

An overview of the reaction path for H/D exchange

The entire path for H/D exchange, presented in Fig. 9, has a mirror element that goes through the η^2-alkane transition state. The first part (A) includes the insertion of the olefin into the Ir–H bond and the coupling of the ethyl and hydride to form the alkane. In the second part (B), a C–H bond of the alkane is cleaved to form an ethyl hydride complex, which itself β-eliminates an olefin. The key characteristic of this entire path is the presence of two steps that are equally important for determining the kinetics of the reaction: the first is reached from the ethyl hydride complex, **7κ^{1}Y′**, going to the alkane transition state [**TS(8-8′)**] in part A and the second is reached from the same **7κ^{1}Y′** going to the β-elimination transition state **TS(5t-7κ^{1}T′)** in part B. These two steps are energetically comparable since they necessarily start from the same alkyl complex **(7κ^{1}Y′)** and go to transition states that are of

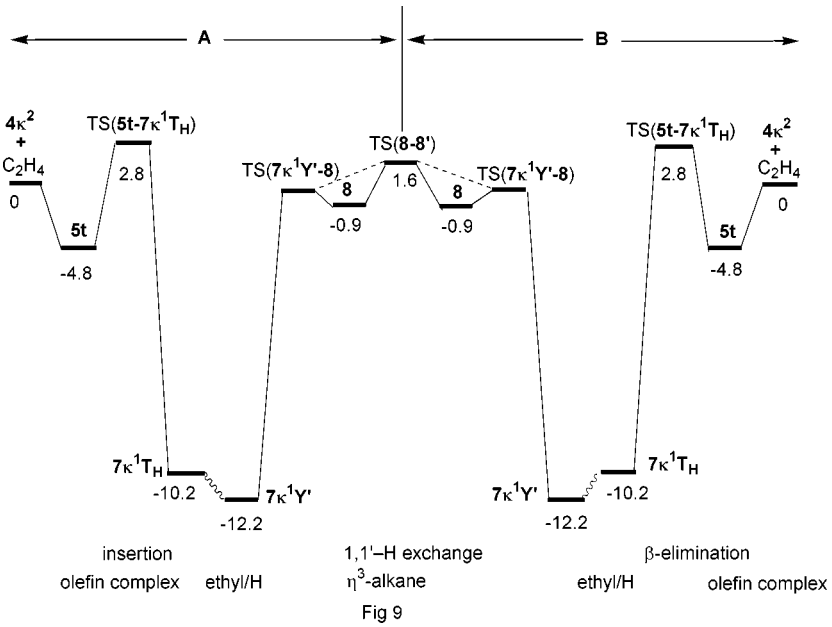

Fig 9

Fig. 9 Full energy profile (kcal mol^{-1}) for 1,1′-H exchange in ethylene in the presence of $IrH_2(tfa)(PH_3)_2$. The energy reference corresponds to separated reactants $IrH_2(tfa)(PH_3)_2$ and C_2H_2 in their optimized geometries. The dotted line indicates that structure **8** may not be a true minimum. Prime should be assumed on the right hand side of the diagram, since B is the mirror image of A.

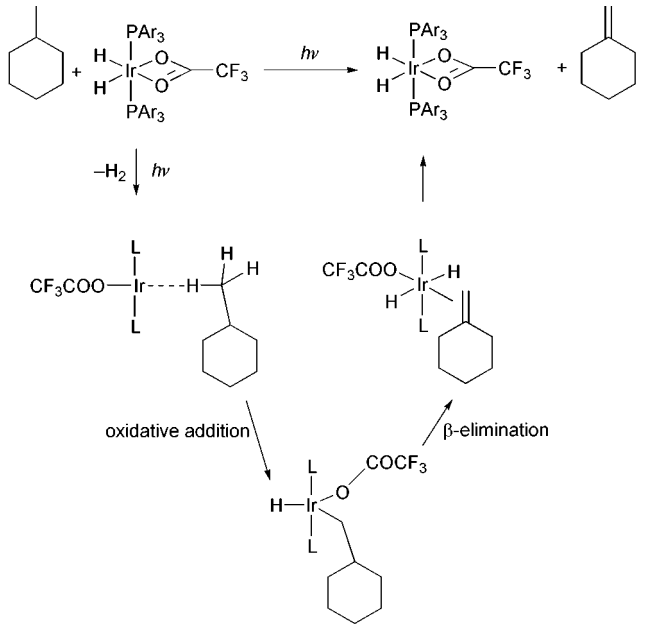

Fig. 10 The mechanism for photochemical alkane dehydrogenation with $Ir(H)_2(tfa)(PAr_3)_2$. The structures shown are schematic and are not intended to represent preferred geometries.

similar energies. The multistep nature of this reaction contrasts with the case of $IrH_5(PCy_3)_2$ where the rate determining step is believed to be the oxidative addition of the C–H bond to the Ir^IHL_2 fragment. The multistep nature of the present reaction prevents any simple interpretation of the experimental isotope effect, k_H/k_D. The observed difference in the values (2.5 in this work and 4.5 under different experimental conditions[33b]), however, is consistent with different mechanisms in these two sets of experiments.

Relation between isotope exchange and alkane dehydrogenation

Mechanism of photochemical alkane dehydrogenation. We originally investigated the H/D exchange reactions in the hope of using the results to understand the alkane functionaliztions of eqn. (1) and (2). This is possible because the isotope exchange is very closely related mechanistically to alkane dehydrogenation with $[IrH_2(PR_3)_2(O_2CCF_3)]$ [eqn. (1) and (2)] since both reactions involve the same intermediates. For example, Fig. 10 shows the path proposed for the photochemical alkane dehydrogenation *via* eqn. (1). The three proposed intermediates involved are precisely those that take part in the H/D exchange process.

In the photochemical version [eqn. (1)], carried out in alkane solution at room temperature, irradiation of starting material **1** at 254 nm leads to conversion of cyclohexane to cyclohexene and methylcyclohexane to methylenecyclohexane and 1-methylcyclohexene (55 : 45 ratio). We interpret the photochemical step as the photoextrusion of H_2, well known in similar systems.[9a] The resulting Ir(I) fragment can then bind alkane to give the same alkane complex as we saw in Fig. 6. The reaction to release alkene can then proceed as discussed above and shown in Fig. 9. The crucial difference between this reaction and the dehydrogenation catalyzed by $[(PCP)Ir(H)_2]$[18] is that initial extrusion of H_2 permits the reaction to go downhill from the alkane adduct to the olefin complex. The experimental product ratio indicates that the 14e Ir(I) intermediate in this reaction slightly prefers to bind methylcyclohexane by the less hindered methyl group. The preferential formation of methylenecyclohexane indicates that Ir(I) attacks the alkane at the methyl group to give the primary alkyl after oxidative addition. Any other attack would tend to give the much stabler 1-methylcyclohexene.

Mechanism of thermal alkane dehydrogenation. In the thermal version of the reaction (Fig. 11), $^tBuCH{=}CH_2$ dehy-

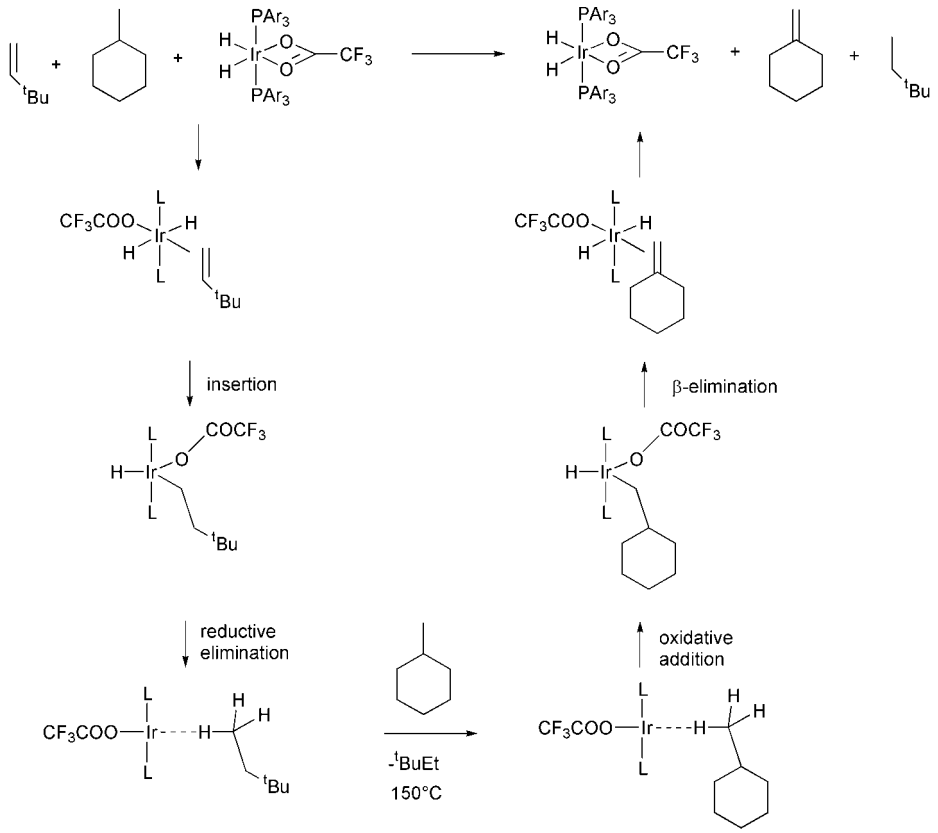

Fig. 11 The mechanism for thermal dehydrogenation of alkanes with $Ir(H)_2(tfa)(PAr_3)_2$. The structures shown are schematic and are not intended to represent preferred geometries.

drogenates the starting metal dihydride complex, **1**. The first part of the reaction is predicted to go uphill from the $^{t}BuCH{=}CH_2$ adduct to the $^{t}BuCH_2CH_3$ complex. Substitution of the alkane is achieved as a result of the high temperature in the reaction (150 °C) and is probably helped by the presence of the bulky ^{t}Bu group. Once substitution of the alkane occurs, the second part of the reaction is downhill from the methylcyclohexane adduct to the methylenecyclohexane adduct. The knowledge gained from the isotope exchange studies above thus allows us to suggest that the $^{t}BuCH_2CH_3$ complex of Ir(tfa)L_2 is a likely intermediate instead of **4κ**^{1} and that a much higher temperature is evidently required, not for the C–H activation step (which the calculations suggest has no activation energy), as might have been assumed, but to cause substitution of the reagent-derived alkane, $^{t}BuCH_2CH_3$ to give the methylcyclohexane adduct. Since the BDE of the alkane in [(alkane)IrXL_2] is calculated to be lower when X = H, rather than X = tfa, it should be easier to decoordinate the alkane in the case of X = H. In agreement with this step being rate determining, a much lower reaction temperature (100 *vs.* 150 °C) was reported for alkane dehydrogenation with $[IrH_5(P^{i}Pr_3)_2]$/$^{t}BuCH{=}CH_2$ than with the present tfa system.[51]

Conclusions

A re-examination of the mechanism of H/D olefin exchange in the presence of $Ir(H)_2(O_2CCF_3)(PAr_3)_2$ *via* a combined experimental and theoretical approach leads to the proposal that the preferred route goes *via* a transition state having an alkane coordinated through two C–H bonds (Fig. 8). After opening of the tfa chelate ring, an easy process, the alkene coordinates. Indeed, the whole pathway seems to go through κ^1-tfa species. Insertion cannot occur from the most stable olefin complex, but only from a *trans* dihydride isomer in which the M–H bond is more nucleophilic. Rather than α-elimination to give the carbene, experimental and theoretical data suggest that the alkyl hydride prefers to reductively eliminate to give a bound alkane TS. The unusually strong binding in the TS accounts for the lack of free alkane as product and may contribute to the much higher barrier calculated for the 1,3- *vs.* the 1,1′-migration in the alkane complex. Rather than the carbene mechanism previously invoked, a sticky alkane route could explain the finding[32] of preferential 1,1′-polydeuteration of alkanes by Pt(II)/DOAc.

These results suggest that it is the presence of the tfa ligand that allows the Ir fragment to bind the alkane so strongly. This allows the H/D exchange to occur without alkane decoordination. The hemilabile character of tfa allows coordination of $^{t}BuCH{=}CH_2$. The tfa also *indirectly* inhibits the vinyl C–H oxidative addition, a process that is not feasible on the Ir(III) starting material even if the tfa is monodentate and not feasible at the Ir(I) stage because no exchangeable D atoms are left bound to the metal.

These results permit us to unify the mechanism of alkane dehydrogenation with that for H/D atoms exchange in olefins by $IrH_2(O_2CCF_3)(PAr_3)_2$. In the alkane dehydrogenation the two H ligands of the catalyst are removed either by photoextrusion or by transfer to a hydrogen acceptor olefin. The catalytic reaction only occurs at 150 °C, because only then does thermal substitution of the alkane derived from the hydrogen acceptor becomes possible. After dissociation of this alkane, the resulting highly reactive species, *trans*-$Ir(O_2CCF_3)(PAr_3)_2$, is proposed to coordinate the substrate alkane, which is then dehydrogenated. The 14e species is not formed in the H/D exchange reaction, however, where the acceptor alkane acts as protecting group. This study not only unifies reactions previously regarded as distinct but it also shows that combining calculations with experiment can suggest answers to chemical problems even where intermediates defy experimental detection.

Technical section

Computational details

The calculations were carried out using the GAUSSIAN 98 set of programs[52] within the framework of DFT at the B3PW91 level of the theory.[53,54] Extra calculations were also carried out using the LYP correlation functional.[55] Ir was represented using the Hay–Wadt relativistic electron core potential (ECP) for the 46 innermost electrons and its associated double ζ basis set.[56,57] Cl and P were also represented with the Los Alamos ECPs and their associated double ζ augmented by a d polarization function.[58] A 6-31G(d,p) basis set was used for all other atoms.[59] This basis set has been used for a large number of similar studies and gives a proper description of bonding in organometallic species.[60] The BSSE correction is not calculated since it has been shown to be small with DFT calculations and this basis set.[60] Full optimizations without symmetry constraints have been carried out. The nature of all transition states was assigned by analytical frequency calculations. ZPE corrections were calculated for each extrema. The corresponding values are given on the figures but discussion has been limited to cases where it had an influence. The transition state structures were slightly perturbed then further geometrically optimized to ensure they connect the reactant and product of interest.

Experimental details

Syntheses were carried out under purified N_2 or Ar as described in before.[33b] NMR spectra were obtained on Bruker WM500, HX490, GE-Omega 300 and WM250 instruments and IR spectra on a Nicolet 5-SX FT-IR. Dideuteriomethylenecyclohexane ($C_6H_{10}CD_2$) was prepared from cyclohexanone (Aldrich) and Ph_3PCD_2 by the literature method[37b,c] and purified using a GOW-MAC series 350 gas chromatograph. Other materials were obtained from Aldrich Chemical Co. and Strem Chemical Co. and purified by standard techniques.

NMR observation of deuteriation. In a typical case, d^2-**1** (Ar = *p*-FC_6H_5; 35 mg, 0.037 mmol) was dissolved in C_6H_6 (0.5 mL) and alkene (3 mol equiv.) added by syringe in an NMR tube under Ar. The reaction was monitored by ^{2}H NMR over 3 h. Monitoring the ^{31}P resonances allowed quantification of the metal complexes present [orthometallated complex: +17.1, −44.3 ppm; phenyl hydride: +17.2 or +17.3 ppm (C_6D_5 form)] relative to a known concentration of an external PPh_3 standard. The authentic compounds were used to identify the resonances. In all cases, D incorporation happened at essentially the same rate in all the vinylic hydrogen positions and for all the alkenes. Alkane was not a significant product (<5%) in any case. Isomerization of the C=C double bond was significant only for $PhCH_2CH{=}CH_2$; in other cases it was <5%. GC-MS showed that the labeled alkene was *ca.* 85% d^2 for the monosubstituted alkenes and d^1 for the 1,1-disubstituted alkenes. The results were independent of solvent (benzene, toluene, dichloromethane). Kinetic isotope effects were determined by ^{2}H-NMR spectroscopy using five determinations over the first 10% of reaction, where product formation is essentially linear with time.

Study of k_{CH}/k_{CD} for Ir–D/$C_6H_{10}CH_2$ *vs.* Ir–H/$C_6H_{10}CD_2$ exchange. To determine k_{CH}, d^2-**1** (Ar = *p*-FC_6H_5; 35 mg, 0.037 mmol) was dissolved in C_6H_6 (0.5 mL) and $C_6H_{10}CH_2$ (20 mol equiv) added by syringe in an NMR tube under Ar. The reaction was monitored by ^{2}H NMR over 2 h at 20 °C.

The value of k_{CD} was determined similarly by following the reaction of **1** (20 mg, 0.02 mmol) with $C_6H_{10}CD_2$ (20 mol equiv.) in C_6D_6 (0.5 mL) at 20 °C *via* ^{1}H NMR over 2 h. Thirty data points were taken and analyzed by the GE-Omega kinetics program.

Acknowledgements

We thank Dr Mark Burk for initiating work in this area, which was supported by the NSF (R. H. C.), the DOE (D. H. L.), University Montpellier 2 and the CNRS (H. G., O. E.).

References

1 S. E. Bromberg, H. Yang, M. C. Asplund, T. Lian, B. K. McNamara, K. T. Kotz, J. S. Yeston, M. Wilkens, H. Frei, R. G. Bergman and C. B. Harris, *Science*, 1997, **278**, 260.
2 T. A. Mobley, C. Schade and R. G. Bergman, *J. Am. Chem. Soc.*, 1995, **117**, 7822.
3 R. N. Perutz and J. J. Turner, *Inorg. Chem.*, 1975, **14**, 262.
4 C. E. Brown, Y. Ishikawa, P. A. Hackett and J. Rayner, *J. Am. Chem. Soc.*, 1990, **112**, 2530.
5 (*a*) C. Hall and R. N. Perutz, *Chem. Rev.*, 1996, **96**, 3125; (*b*) A. E. Shilov and G. B. Shul'pin, *Chem. Rev.*, 1997, **97**, 2879.
6 R. H. Crabtree, *Chem. Rev.*, 1995, **95**, 987.
7 R. H. Crabtree, *Angew. Chem., Int. Ed. Engl.*, 1993, **32**, 789.
8 B. K. McNamara, J. S. Yeston, R. G. Bergman and C. B. Moore, *J. Am. Chem. Soc.*, 1999, **121**, 6437.
9 (*a*) R. A. Periana and R. G. Bergman, *J. Am. Chem. Soc.*, 1986, **108**, 7332; (*b*) P. J. Alaimo and R. G. Bergman, *Organometallics*, 1999, **18**, 2707; (*c*) D. D. Wick, K. A. Reynolds and W. D. Jones, *J. Am. Chem. Soc.*, 1999, **121**, 3974; (*d*) S. S. Stahl, J. A. Labinger and J. A. Bercaw, *J. Am. Chem. Soc.*, 1996, **118**, 5961; (*e*) D. F. Schafer and P. T. Wolczanski, *J. Am. Chem. Soc.*, 1998, **120**, 4881; (*f*) J. C. Green and C. N. Jardine, *J. Chem. Soc., Dalton Trans.*, 1998, 1057; (*g*) L. Johansson, M. Tilset, J. A. Labinger and J. E. Bercaw, *J. Am. Chem. Soc.*, 2000, **122**, 10846.
10 (*a*) D. W. Lee and C. M. Jensen, *J. Am. Chem. Soc.*, 1996, **118**, 8749; (*b*) R. N. Perutz and J. J. Turner, *J. Am. Chem. Soc.*, 1975, **97**, 4791; (*c*) D. C. Grills, X. Z. Sun, G. I. Childs and M. W. George, *J. Phys. Chem.*, 2000, **104**, 4300; (*d*) A. Chernega, J. Cook, M. L. H. Green, L. Labella, S. J. Simpson, J. Souter and A. H. H. Stephens, *J. Chem. Soc., Dalton Trans.*, 1997, 3225; (*e*) E. F. Walsh, V. K. Popov, M. W. George and M. Poliakoff, *J. Phys. Chem.*, 1995, **99**, 12016.
11 X. Z. Sun, D. C. Grills, S. Nikiforov, M. Poliakoff and M. W. George, *J. Am. Chem. Soc.*, 1997, **119**, 7521.
12 D. R. Evans, T. Drovetskaya, R. Bau, C. A. Reed and P. D. W. Boyd, *J. Am. Chem. Soc.*, 1997, **119**, 3633.
13 S. Geftakis and G. E. Ball, *J. Am. Chem. Soc.*, 1998, **120**, 9953.
14 S. Geftakis and G. E. Ball, *J. Am. Chem. Soc.*, 1999, **121**, 6336.
15 K. Koga and K. Morokuma, *Chem. Rev.*, 1991, **91**, 823.
16 D. G. Musaev and K. Morokuma, in *Advances in Chemical Physics*, ed. S. A. Rice and I. Prigogine, John Wiley & Sons, New York, NY, 1996, vol. XCV, p. 61.
17 S. Niu and M. B. Hall, *Chem. Rev.*, 2000, **100**, 353.
18 S. Niu and M. B. Hall, *J. Am. Chem. Soc.*, 1999, **121**, 3992.
19 S. Zaric and M. B. Hall, *J. Phys. Chem.*, 1997, **101**, 4646.
20 M. D. Su and S. Y. Chu, *J. Am. Chem. Soc.*, 1997, **119**, 5373.
21 A. J. Lees and A. A. Purwoko, *Coord. Chem. Rev.*, 1994, **132**, 155.
22 K. M. Waltz and J. F. Hartwig, *Science*, 1997, **277**, 211.
23 R. A. Periana and R. G. Bergman, *Organometallics*, 1984, **3**, 508.
24 R. A. Periana, D. J. Taube, S. Gamble, H. Taube, T. Satoh and H. Fujii, *Science*, 1998, **280**, 560.
25 B. A. Arndtsen and R. G. Bergman, *Science*, 1995, **270**, 1970.
26 M. J. Burk, R. H. Crabtree and D. V. McGrath, *J. Chem. Soc., Chem. Commun.*, 1985, 1829.
27 M. J. Burk, D. V. McGrath and R. H. Crabtree, *J. Am. Chem. Soc.*, 1988, **110**, 620.
28 R. M. Bullock, C. E. L. Headford, S. E. Kegley and J. R. Norton, *J. Am. Chem. Soc.*, 1985, **107**, 727.
29 G. L. Gould and D. M. Heinekey, *J. Am. Chem. Soc.*, 1989, **111**, 5502.
30 C. L. Gross and G. S. Girolami, *J. Am. Chem. Soc.*, 1998, **120**, 6605.
31 R. L. Martin, *J. Am. Chem. Soc.*, 1999, **121**, 9459.
32 A. E. Shilov and G. B. Shul'pin, *Activation and Catalytic Reactions of Saturated Hydrocarbons in the Presence of Metal Complexes*, Kluwer, Dordrecht, 2000, p. 267 ff.
33 (*a*) J. W. Faller and H. Felkin, *Organometallics*, 1985, **4**, 1488; (*b*) M. J. Burk and R. H. Crabtree, *J. Am. Chem. Soc.*, 1987, **109**, 8025.
34 Y. Jean and O. Eisenstein, *Polyhedron*, 1988, **7**, 405.
35 I. E.-I. Rachidi, O. Eisenstein and Y. Jean, *New J. Chem.*, 1990, **14**, 671.
36 J.-F. Riehl, Y. Jean, O. Eisenstein and M. Pélissier, *Organometallics*, 1992, **11**, 729.
37 (*a*) R. H. Schultz, A. A. Bengali, M. J. Tauber, B. H. Weiller, E. P. Wasserman, K. R. Kyle, C. B. Moore and R. G. Bergman, *J. Am. Chem. Soc.*, 1994, **116**, 7369 and references therein; (*b*) G. Wittig and A. Hesse, *Org. Synth.*, 1970, **50**, 66; (*c*) G. W. Guchanan and A. E. Gustafson, *J. Org. Chem.*, 1973, **38**, 2910.
38 (*a*) R. R. Schrock, S. W. Seidel, N. C. Mosch-Zanetti, K. Y. Shih, M. B. O'Donoghue and W. M. Davis, *J. Am. Chem. Soc.*, 1997, **119**, 11871; (*b*) D.-H. Lee, J. Chen, J. W. Faller and R. H. Crabtree, *Chem. Commun.*, 2001, 213.
39 J. N. Coalter, G. J. Spivak, H. Gérard, E. Clot, E. R. Davidson, O. Eisenstein and K. G. Caulton, *J. Am. Chem. Soc.*, 1998, **120**, 9388.
40 J. N. Coalter, J. C. Bollinger, J. C. Huffman, U. Werner-Zwanziger, K. G. Caulton, E. R. Davidson, H. Gérard, E. Clot and O. Eisenstein, *New J. Chem.*, 2000, **24**, 9.
41 M. Loza, J. W. Faller and R. H. Crabtree, *Inorg. Chem.*, 1995, **34**, 2937.
42 D. Huang, H. Gérard, E. Clot, V. Young, Jr., W. E. Streib, O. Eisenstein and K. G. Caulton, *Organometallics*, 1999, **18**, 5441.
43 P. Burger and R. G. Bergman, *J. Am. Chem. Soc.*, 1993, **115**, 10462.
44 R. Jimenez-Cataño and M. B. Hall, *Organometallics*, 1996, **15**, 1889.
45 P. E. M. Siegbahn and R. H. Crabtree, *J. Am. Chem. Soc.*, 1996, **118**, 4442.
46 M. D. Su and S. Y. Chu, *Inorg. Chem.*, 1998, **37**, 3400.
47 S. Sakaki, B. Biswas and M. Sugimoto, *Organometallics*, 1998, **17**, 1278.
48 M. D. Su and S. Y. Chu, *Organometallics*, 1997, **16**, 1621.
49 P. E. M. Siegbahn, *J. Am. Chem. Soc.*, 1996, **118**, 1487.
50 T. R. Cundari, *J. Am. Chem. Soc.*, 1994, **116**, 340.
51 H. Felkin, T. Fillebeen-Khan, R. Holmes-Smith and L. Yingrui, *Tetrahedron Lett.*, 1985, **26**, 1999.
52 M. J. Frisch, G. W. Trucks, H. B. Schlegel, G. E. Scuseria, M. A. Robb, J. R. Cheeseman, V. G. Zakrzewski, J. A. Montgomery, Jr., R. E. Stratmann, J. C. Burant, S. Daprich, J. M. Millam, A. D. Daniels, K. N. Kudin, M. C. Strain, O. Farkas, J. Tomasi, V. Barone, M. Cossi, R. Cammi, B. Mennucci, C. Pomelli, C. Adamo, S. Clifford, J. Ochterski, G. A. Petersson, P. Y. Ayala, Q. Cui, K. Morokuma, D. K. Malick, A. D. Rabuck, K. Raghavachari, J. B. Foresman, J. Cioslowski, J. V. Ortiz, A. G. Baboul, B. B. Stefanov, G. Liu, A. Liashenko, P. Piskorz, I. Komaromi, R. Gomperts, R. L. Martin, D. J. Fox, T. Keith, M. A. Al-Laham, C. Y. Peng, A. Nanayakkara, C. Gonzalez, M. Challacombe, P. M. W. Gill, B. Johnson, W. Chen, M. W. Wong, J. L. Andres, C. Gonzalez, M. Head-Gordon, E. S. Replogle and J. A. Pople, GAUSSIAN 98, Rev. A.7, Gaussian, Inc., Pittsburgh, PA, 1998.
53 A. D. Becke, *J. Chem. Phys.*, 1993, **98**, 5648.
54 C. Lee, W. Yang and R. G. Parr, *Phys. Rev. B*, 1988, **37**, 785.
55 J. P. Perdew and Y. Wang, *Phys. Rev. B*, 1992, **45**, 13244.
56 P. G. Hay and W. R. Wadt, *J. Chem. Phys.*, 1985, **82**, 299.
57 W. R. Wadt and P. G. Hay, *J. Chem. Phys.*, 1985, **82**, 184.
58 A. H. Höllwarth, M. B. Böhme, S. Dapprich, A. W. Ehlers, A. Gobbi, V. Jonas, K. F. Köhler, R. Stegman, A. Veldkamp and G. Frenking, *Chem. Phys. Lett.*, 1993, **208**, 237.
59 P. C. Hariharan and J. A. Pople, *Theor. Chim. Acta*, 1973, **28**, 213.
60 A. Rosa, A. W. Ehlers, E. J. Baerends, J. G. Snijders and G. te Velde, *J. Phys. Chem.*, 1996, **100**, 5690.